Manuscript accepted by Ad Hoc Networks journal, July 2010.

Design and Performance Analysis of MAC Schemes for Wireless Sensor Networks Powered by Ambient Energy Harvesting[☆]

Zhi Ang Eu[a,*], Hwee-Pink Tan[b], Winston K. G. Seah[c]

[a] *NUS Graduate School for Integrative Sciences and Engineering*
National University of Singapore
CeLS, #05-01, 28 Medical Drive, Singapore 117456
[b] *Networking Protocols Department*
*Institute for Infocomm Research (I^2R), A*STAR*
1 Fusionopolis Way, #21-01 Connexis, Singapore 138632
[c] *School of Engineering and Computer Science*
Victoria University, PO Box 600, Wellington 6140, New Zealand

Abstract

Energy consumption is a perennial issue in the design of wireless sensor networks (WSNs) which typically rely on portable sources like batteries for power. Recent advances in ambient energy harvesting technology have made it a potential and promising alternative source of energy for powering WSNs. By using energy harvesters with supercapacitors, WSNs are able to operate perpetually until hardware failure and in places where batteries are hard or impossible to replace. In this paper, we study the performance of different medium access control (MAC) schemes based on CSMA and polling techniques for WSNs which are solely powered by ambient energy harvesting using energy harvesters. We base the study on (i) network throughput (S), which is the rate of sensor data received by the sink, (ii) fairness index (F), which determines whether the bandwidth is allocated to each sensor node equally and (iii) inter-arrival time (γ) which measures the average time difference between two packets from a source node. For CSMA, we compare both the slotted and unslotted variants. For polling, we

[☆] A preliminary version of this paper is published in the Fourth International Wireless Internet Conference (WICON), November 2008

[*] corresponding author, telephone number: +65-64082319
Email addresses: euzhiang@nus.edu.sg (Zhi Ang Eu), hptan@i2r.a-star.edu.sg (Hwee-Pink Tan), Winston.Seah@ecs.vuw.ac.nz (Winston K. G. Seah)

first consider identity polling. Then we design a probabilistic polling protocol that takes into account the unpredictability of the energy harvesting process to achieve good performance. Finally, we present an optimal polling MAC protocol to determine the theoretical maximum performance. We validate the analytical models using extensive simulations incorporating experimental results from the characterization of different types of energy harvesters. The performance results show that probabilistic polling achieves high throughput and fairness as well as low inter-arrival times.
Keywords: Wireless Sensor Networks, Medium Access Control, CSMA, Probabilistic Polling, Energy Harvesting.

1. Introduction

Current research on wireless sensor networks (WSNs) [1], and more recently wireless multimedia sensor networks [2], have focused on extending network lifetime [3] since they are powered using finite energy sources (e.g., batteries). One way to extend the lifetime of sensor networks is to replenish the energy source by replacing batteries. However, physical and environmental constraints may restrict the ability to replace the batteries or retrieve the batteries to do so. Moreover, battery-powered WSNs are inappropriate for some applications due to environmental concerns arising from the risk of battery leakage.

In comparison, in *W*ireless *S*ensor *N*etworks *P*owered by *A*mbient *E*nergy *H*arvesting (which we refer to as WSN-HEAP in this paper), each sensor node is equipped with one or more energy harvesting devices to harvest ambient energy such as light, vibration, heat and wind from the environment, and an energy storage device to store the harvested energy. The main hardware differences between a battery-powered wireless sensor node and WSN-HEAP node are illustrated in Fig. 1.

The energy characteristics of a WSN-HEAP node are different from that of a battery-powered sensor node, as illustrated in Fig. 2. In a battery-powered node, the total energy reduces with time and the sensor node can operate until

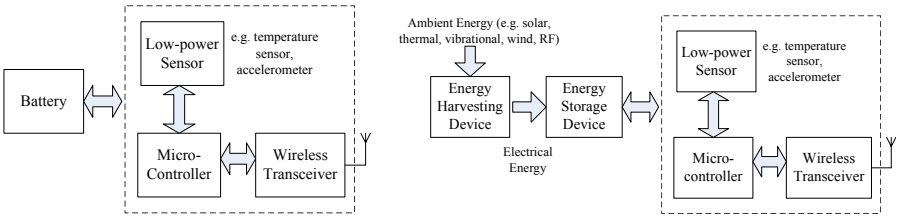

(a) Battery-operated wireless sensor node

(b) WSN-HEAP node

Figure 1: Battery-operated versus energy-harvesting sensor node

the energy level reaches an unusable level. Since the energy harvesting rates achievable with WSN-HEAP devices in the market today are much lower than the power consumption for node operation (sensing, processing and communication), harvested energy is accumulated in a storage device until a certain level before the node can operate. The process is repeated when the energy is depleted, as illustrated in Fig. 3. Since storage devices such as supercapacitors offer virtually unlimited recharge cycles, WSN-HEAP can potentially operate for very long periods of time (years or even decades) without the need to replenish its energy manually.

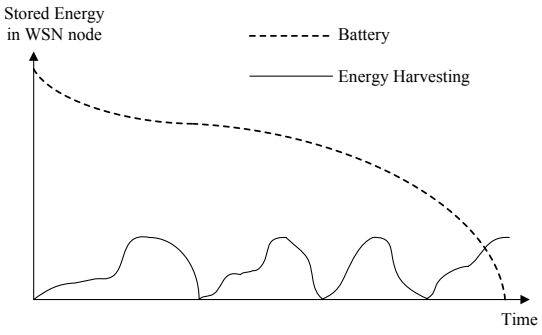

Figure 2: Energy characteristics of different energy sources

The above characteristics of WSN-HEAP render it suitable for many sensing applications including structural health monitoring ([4],[5]), where (i) energy may be harvested from ambient sources (e.g., vibration, light, heat, wind) to

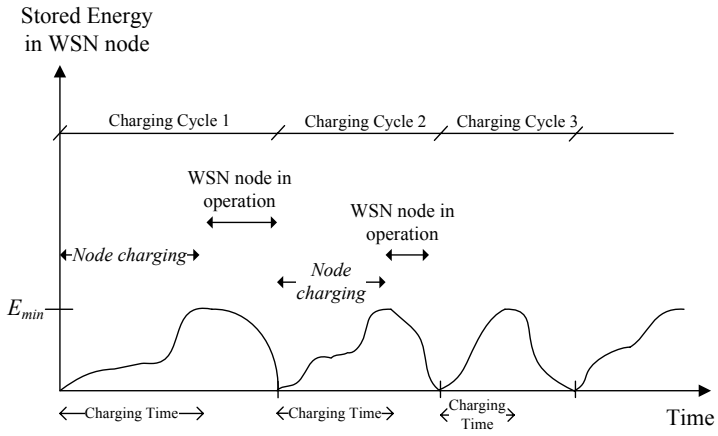

Figure 3: Charging cycles of WSN-HEAP nodes

power each device; (i) monitoring is active (i.e., data is sensed periodically by each node and forwarded to the sink); and (iii) it is often infeasible (with sensors embedded into structures in buildings) or hazardous (with sensors welded into structures at construction sites) to replace batteries.

To achieve adequate, fair and timely monitoring, appropriate medium access control (MAC) is needed to coordinate the transmission of each WSN-HEAP node. The main challenge is that the time taken to charge up the sensor node to a useful level varies because of environmental factors as well as the type and size of the energy harvesters used. Moreover, WSN-HEAP nodes are only awake intermittently and for a short period of time. These unique characteristics render the direct application of many MAC protocols proposed for battery-powered WSNs unsuitable or non-optimal for use in WSN-HEAP.

In this paper, we consider MAC protocols for WSN-HEAP. This paper has two main contributions. The first main contribution is the performance analysis of existing MAC schemes when adapted for use in WSN-HEAP in a single-hop scenario. Our analysis focuses on (i) network throughput (S), which is the rate at which the sink receives data from all the sensor nodes; (ii) fairness (F), which determines if each node receives an equal share of the bandwidth; and (iii) inter-arrival time (γ), which gives the average time delay between the arrival of two

successive packets from the same source at the sink. Our analysis uses the average value of a variable (e.g. average charging rate) wherever possible which is a methodology commonly used in the performance analysis of computer systems. This is because from our empirical measurements, the energy charging characteristics do not follow well-known statistical distributions that lead to tractable analysis, therefore using stochastic analysis is difficult. We validate our analysis by comparing numerical predictions with simulation results using empirical charging times taken from our experiments. The second contribution is the design and analysis of a probabilistic polling algorithm that specifically exploits the unpredictability of the energy harvesting process to achieve high throughput and fairness as well as low inter-arrival times in WSN-HEAP. We validate our analytical models by comparing the numerical predictions with simulation results. To the best of our knowledge, our work is the first comprehensive study of the impact of different MAC protocols on network performance in wireless sensor networks that are solely powered using energy harvesters.

The rest of this paper is organized as follows: In Section 2, we review some work on energy harvesting technologies and their application in sensor networks, as well as MAC protocols. In Section 3, we empirically characterize commercial energy harvesting devices in order to derive realistic deployment scenarios as well as traffic and energy models for WSN-HEAP. We also present relevant performance metrics, as well as various CSMA-based and polling-based MAC protocols for WSN-HEAP in Section 4. Next, we design an improved form of polling using probabilistic methods in Section 5. The performance results and comparison of various MAC protocols are presented in Section 6. We conclude the paper in Section 7. The notations used in this paper are summarized in Table 1.

2. Related Work

Most sensor nodes used in WSNs today rely on a limited energy source like primary batteries to operate. One attempt [6] to solve the energy problem

Table 1: Notations used in the paper

Symbol	Denotes
E_{rx}	Energy required to receive a data packet
E_{ta}	Energy required to change state (from receive to transmit or from transmit to receive)
E_{tx}	Energy required to send a data packet
E_f	Energy of a fully charged sensor node
F	Fairness
n	Number of sensor nodes in the network
p_c	Contention probability in probabilistic polling
P_{rx}	Power needed when the sensor is in receive state
P_{ta}	Power needed to switch from receive to transmit or from transmit to receive
P_{tx}	Power needed when the sensor is in transmit state
R	Per-node throughput of each sensor
S	Network throughput
s_{ack}	Size of an acknowledgment packet from the sink
s_d	Size of a data packet
s_p	Size of a polling packet
t_{cca}	Time taken to determine whether the channel is clear or not
t_{poll}	Time to send a polling packet
t_s	Time of a transmission slot in the slotted CSMA model
t_{tx}	Time to send a data packet
t_{rx_tx}	Hardware turnaround time from receive state to transmit state
t_{tx_rx}	Hardware turnaround time from transmit state to receive state
α	Transmission rate of the sensor
λ	Average energy harvesting rate
γ	Average inter-arrival time between packets from the same source

is to make use of some mobile sensor nodes to deliver energy to other sensor nodes. Another solution that has been adopted is to make use of sensor nodes that rely on energy harvesting devices ([7],[8]) for power. Combining low-power electronics, energy harvesting devices and supercapacitors, it is possible to implement WSN-HEAP in applications like structural health monitoring of civil infrastructures, where the sensors need to be embedded and operate for very long durations, from years to decades.

Some examples of sensor nodes using energy harvesters have been deployed in testbeds. For example, in [9], 557 solar-powered sensor nodes have been used to evaluate robust multi-target tracking algorithms. Other solar-powered sensor network testbeds are illustrated in [10] and [11]. Energy harvesting wireless sensors have also been developed for monitoring the structures of aircraft [12]. There are also commercially available sensor nodes which rely on ambient energy harvesting for power. The devices developed by Microstrain [13] harvest and use energy from two sources, viz. solar and mechanical energy.

To date, none of these efforts address issues related to the networking aspects of WSNs. Instead, the focus is on the efficiency and viability of the energy harvesting method. Furthermore, most of the reported work focused on harvesting energy to supplement battery power while we focus on using the harvested energy as the only energy source. However, for interrupt-driven or event-driven WSN applications, it might not be practical in some scenarios to depend solely on the energy harvester alone. In these scenarios, the energy harvester is used only to recharge the battery when energy is available from the environment. Our work on probabilistic polling is also applicable to these scenarios when the nodes wake up asynchronously to report readings to the sink.

While many MAC protocols have been designed for wireless sensor networks, they are not optimized for the energy characteristics of WSN-HEAP where nodes cannot control their wakeup schedules as the energy charging times are dependent on environmental conditions. Wireless MAC protocols can be classified into two categories, centralized MAC with a coordinator and distributed MAC. Centralized MAC protocols, like polling ([14],[15]), require a centralized coor-

dinator to determine the order of transmissions. Distributed MAC protocols like CSMA require nodes to coordinate the transmissions among themselves. In [16], sleep and wakeup schedules are proposed to reduce energy usage and prolong network lifetime at the expense of longer delays. Since these schemes assume the use of batteries in their scenarios, energy conservation therefore is a key consideration. Sleep and wakeup algorithms have also been designed for sensor networks with energy harvesters. The performance of different sleep and wakeup strategies based on factors such as channel state, battery state and environmental factors are analyzed in [17] and game theory is used to find the optimal parameters for a sleep and wakeup strategy to tradeoff between packet blocking and dropping probabilities [18]. However, they assume the use of a TDMA-based wireless access system and the impact of different MAC protocols on network performance is not analyzed.

Sift [19] is another protocol designed for event-driven sensor networks to minimize collisions in a slotted CSMA system. Another class of MAC protocols which use code assignments is used in DS-UWB wireless networks [20]. However, code assignment as well as the complexity of encoding and decoding are open problems in sensor networks with limited processing resources. An optimal transmission policy [21] can be used to achieve better performance when the data generated is of different priorities.

Our approach differs in the following ways: (i) we consider active monitoring where each sensor node has equal priority and would send sensor data to the sink whenever it accumulates enough energy, making Sift unsuitable for use in our scenario; (ii) in our scenario, ambient energy is harvested which makes the optimal use of this ambient energy to maximize throughput and minimize delays, instead of energy conservation, our key considerations; (iii) we conduct an empirical characterization of energy harvester sensor devices, and demonstrate that energy harvesting times exhibit temporal and spatial fluctuations, are spatially and temporally uncorrelated, are technology-dependent, and duty cycles are very low (less than 10 %). The latter observation renders predictive approaches needed in sleep and wakeup algorithms difficult to realize in practice.

In [22], we evaluated various CSMA-based and polling-based MAC protocols in terms of throughput, and proposed a probabilistic polling mechanism to overcome the limitations of the former protocols in WSN-HEAP. We extend the work in this paper by (i) considering fairness; (ii) investigating the impact of the maximum backoff window on unslotted MAC; (iii) deriving the upper-bound on the achievable performance of polling schemes; and (iv) providing a more in-depth analysis of probabilistic polling and the performance trade-offs with other schemes, based on simulation parameters obtained from empirical characterization of commercial energy harvesting nodes.

3. Characterization of WSN-HEAP

In this paper, our main focus is to develop and evaluate MAC protocols for WSN-HEAP for active monitoring applications such as structural health monitoring. For an accurate evaluation, we first need to define a realistic model for WSN-HEAP. We do so by empirically characterizing the (i) radio behavior as well as (ii) traffic and energy harvesting characteristics of solar [23] and thermal [24] energy harvesting nodes that use the MSP430 microcontroller and CC2500 radio transceiver from Texas Instruments (TI), as shown in Fig. 4.

The sensor node development kit [23] we use consists of a solar panel optimized for indoor use, two eZ430-RF2500T target boards and one AAA battery pack. The target board comprises the TI MSP430 microcontroller, CC2500 radio transceiver and an on-board antenna. The CC2500 radio transceiver operates in the 2.4GHz band with data rate of 250 kbps and is designed for low power wireless applications. The harvested energy is stored in EnerChip, a thin-film rechargeable energy storage device with low self-discharge manufactured by Cymbet.

The experimental setup comprises one or more transmitters (with transmission power fixed at 1dBm) and a receiver (sink) connected to a laptop as shown in Fig. 5a and 5b. The battery pack is used for powering the target board at the transmitter in the radio characterization tests. For the traffic and energy

characterization, a TI evaluation board is used at the receiver as a sniffer to overhear packet transmissions from the transmitter and record their timings accurately.

(a) Outdoor Solar Energy Harvester (b) Indoor Solar Energy Harvester (c) Thermal Energy Harvester

Figure 4: Energy harvesting sensor nodes using MSP430 microcontroller and CC2500 transceiver from Texas Instruments

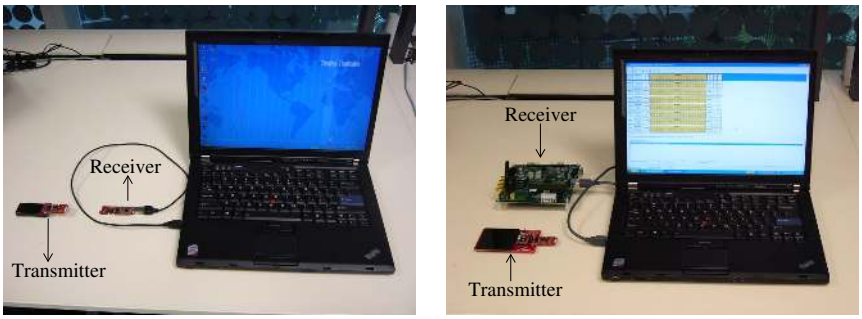

(a) Setup for link measurements (b) Setup for energy measurements

Figure 5: Experimental setup

3.1. Radio Characterization

To quantify the maximum transmission range, we transmit 1000 packets in an open field using the experimental setup shown in Fig. 6a, and measure the ratio of successful receptions (packet delivery ratio or PDR) at different transmitter-receiver distances. Each packet consists of 40 bytes of data (the current maximum value allowed due to software issues) with an additional 11 bytes of headers, therefore each data packet is 51 bytes. The results are shown in Fig. 6b.

To reduce the physical layer overhead, we may want to increase the size of the data packet. Using bit error rate (BER) at different transmitter-receiver distances from the empirical measurements, we can obtain the PDR and transmission range for different packet sizes. For example, the PDR results for 100 bytes packets are shown in the same graph. Although the observed PDR at shorter transmitter-receiver distances is sometimes lower than that at longer distances, the general trend is that the PDR (link quality) degrades gradually with distance, but falls sharply beyond 70m.

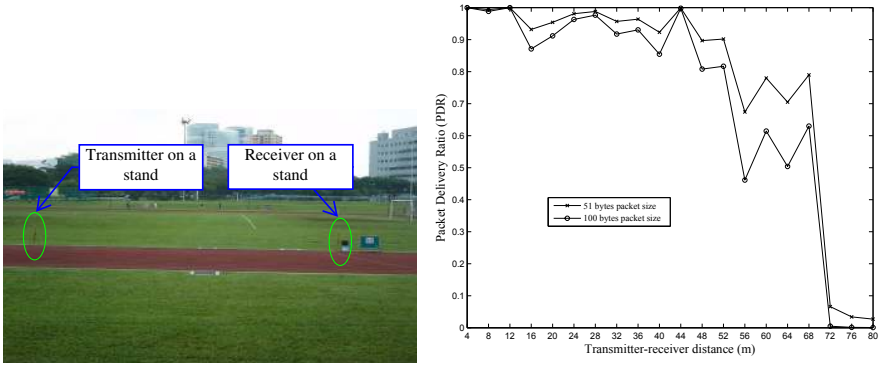

(a) Deployment (b) Results

Figure 6: Radio characterization in open field

3.2. Traffic and Energy Characterization

When the transmitter is powered by the solar or thermal energy harvester, its stored energy is low initially. After some energy harvesting (charging) time, when enough energy has been harvested and accumulated in the energy storage device, the power supply for the microcontroller and transceiver will be switched on. Then, the transmitter will continuously broadcast data packets until the energy is depleted after which the microcontroller and transceiver will be turned off. The energy storage device will start to accumulate energy again and the process is repeated in the next cycle as illustrated in Fig. 3.

We characterize the traffic and energy model of each harvesting device by deploying the setup in various scenarios and recording the charging time as well

as the number of packets transmitted in each cycle. Some of the scenarios that we use are shown in Table 2.

Table 2: Scenarios for characterization of traffic and energy model

Scenario No	Type of Energy Harvester	Location
1	Outdoor Solar	Outdoors, 10am (Average light intensity of 27000 lux)
2	Outdoor Solar	Outdoors, 11am (Average light intensity of 42000 lux)
3	Indoor Solar	Directly under a 28 W fluorescent lamp (Light intensity of 20000 lux) (Fig. 7a)
4	Indoor Solar	1m under a 28W fluorescent lamp (Light intensity of 1600 lux)
5	Indoor Solar	2m under a 28W fluorescent lamp (Light intensity of 700 lux)
6	Thermal	Mounted on a CPU heat sink inside a computer (Fig. 7b) (Temperature gradient of 45°C)

Fig. 8 illustrate the probability density functions (pdf) of the charging times under different scenarios obtained from 1000 charge cycles. The pdf describes the relative likelihood for the charging time to occur within a given time interval and the probability in any time interval is given by the integral of its density over the interval. The number of transmitted packets per cycle (n_{pkt}) ranges from 17 to 19 packets with an average of 17.97 packets. For the outdoor solar energy harvester, the average charging time decreases when light intensity increases (Scenario 2). For the indoor solar energy harvester, the results show that there is greater variation (higher standard deviation) in the charging time required for each charge cycle when the sensor node is further away from the light source. A summary of the energy harvesting characteristics obtained from these experiments is given in Table 3. The bin size refers to the data range for

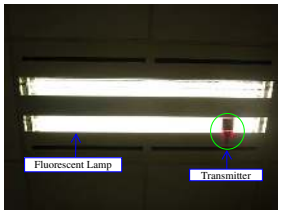

(a) Solar Energy Harvester under a fluorescent lamp

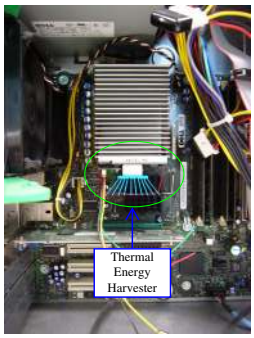

(b) Thermal Energy Harvester mounted on a CPU Heat Sink

Figure 7: Placement of energy harvesters for energy measurements

each interval for the histogram. It depends on minimum and maximum charging time as well as the number of intervals required. We have chosen the bin size such that the distribution of the charging time can be observed clearly from the histogram. The duty cycle (κ) refers to the time in which the node is in active state where it is transmitting data packets. It can be computed by

$$\kappa = \frac{n_{pkt} t_{tx}}{n_{pkt} t_{tx} + t_c} \tag{1}$$

where n_{pkt} is the average number of packets transmitted per charging cycle, t_c is the average charging time for each cycle and t_{tx} is the time taken for a packet transmission. For a packet size, s_d, of 51 bytes used in our radio characterization tests, and data rate, α of 250 kbps, the packet transmission time, t_{tx} is 1.632 ms. The energy harvesting rate can be obtained by considering the total energy consumed during node operation given by

$$E_{total} = n_{pkt} P_{tx} t_{tx}. \tag{2}$$

Then the energy harvesting rate can be computed using

$$\lambda = \frac{E_{total}}{t_c + n_{pkt} t_{tx}}. \tag{3}$$

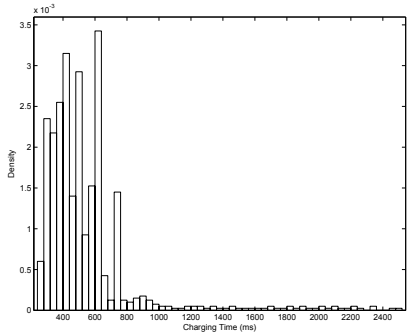

(a) Outdoor solar energy harvester at 10am

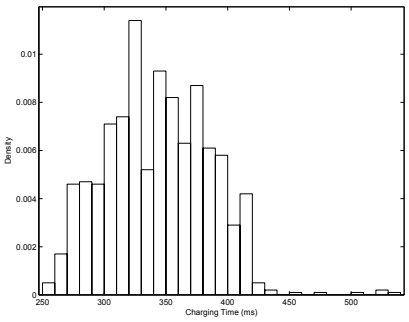

(b) Outdoor solar energy harvester at 11am

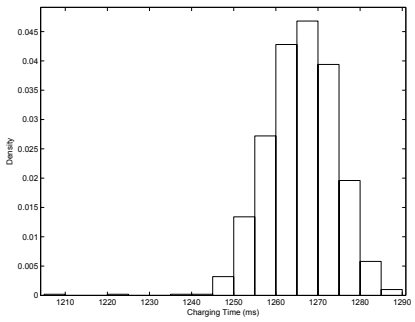

(c) Solar energy harvester directly under fluorescent lamp

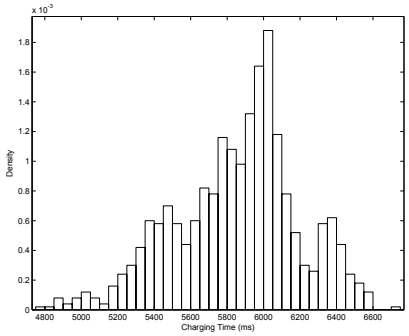

(d) Solar energy harvester 1m under fluorescent lamp

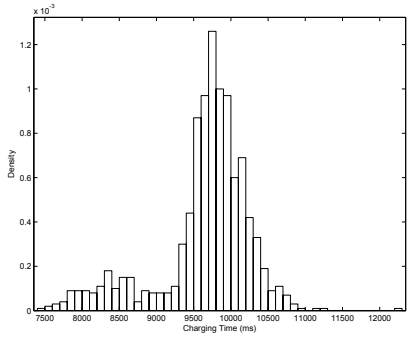

(e) Solar energy harvester 2m under fluorescent lamp

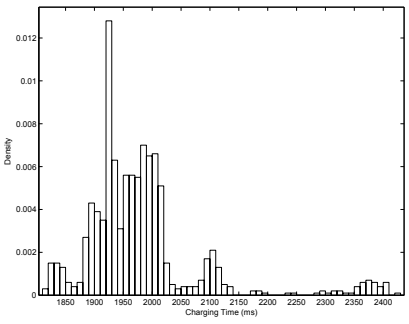

(f) Thermal energy harvester on a CPU heat sink

Figure 8: Probability density functions of charging times in different scenarios

Table 3: Charging Time Statistics for scenarios 1 to 6

	Scenario 1	Scenario 2	Scenario 3
Minimum Charging time (ms)	270.27	257.01	1208.63
Maximum Charging time (ms)	2518.26	538.32	1286.12
Average Charging time (ms), t_c	547.23 m	343.31	1266.10
Standard deviation (ms)	309.63	41.94	8.12
Bin size in Fig. 8 (ms)	40	10	5
Average time to harvest energy to send one packet (ms)	30.45	19.10	70.46
Duty cycle (%)	5.09	7.87	2.26
Average energy harvesting rate (mW)	4.75	7.35	2.11

	Scenario 4	Scenario 5	Scenario 6
Minimum Charging time (ms)	4753.88	7470.19	1818.71
Maximum Charging time (ms)	6734.70	12279.66	2422.81
Average Charging time (ms), t_c	5854.37	9655.25	1980.46
Standard deviation (ms)	340.34	623.37	105.14
Bin size in Fig. 8 (ms)	50	100	10
Average time to harvest energy to send one packet (ms)	325.79	537.30	110.21
Duty cycle (%)	0.50	0.30	1.46
Average energy harvesting rate (mW)	0.47	0.28	1.36

Upon visual inspections, the histograms suggest that the distributions can be modeled using normal distributions. We carry out statistical tests using the chi-square goodness-of-fit test [25]. We divide the data into 52 (exponential) or 53 intervals (uniform and normal) so that the degrees of freedom is 50. At the 0.05 level of significance, the critical value $\chi^2_{0.05,5}$ is 67.5. The null hypothesis that the charging time conforms to the distributional assumption is rejected if the computed χ^2 value exceeds 67.5. Other than testing for normal distribution, we also compute the χ^2 values for exponential and uniform distributions as shown in Table 4. As expected, the χ^2 values for exponential and uniform are large, indicating that they do not fit these distributions at all. The χ^2 values for the normal distribution are smaller, however only scenario 3 fits the normal distribution from the statistical tests. Therefore, since the empirical measurements do not fit any of these well-known distributions well, we have used actual charging time measurements in our simulations to reflect actual performance.

Table 4: χ^2 values for different scenarios

Scenario	Uniform Distribution	Exponential Distribution	Normal distribution
Scenario 1	3782.9	2047.0	1307.4
Scenario 2	990.9	5239.0	154.2
Scenario 3	1757.6	38239.9	32.4
Scenario 4	842.7	12364.7	164.8
Scenario 5	2340.8	14634.0	2428.1
Scenario 6	2227.2	20250.9	731.2

Next, we investigate the temporal and spatial variation of energy harvesting, and quantify the level of time correlation in charging time across charging cycles.

- **Temporal variation:**

  For scenario 1, we plot the average energy harvesting rate obtained at 1-minute intervals for measurements collected over 30 minutes in Fig. 9.

The light intensity during this period was from 5000 lux to 40000 lux. We observe that the average energy harvesting rate changes over time, decreasing (increasing) when light intensity decreases (increases).

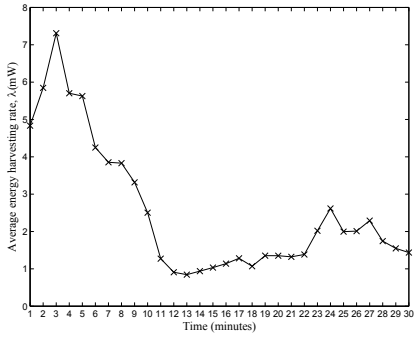

Figure 9: Average charging times of the node in different time intervals

- **Spatial variation:**

  For scenarios 1 and 4, we fixed the position of one node, and position the second node within a radius of 1m. For each placement, we compute the average harvesting rate over 10 minutes, and plot them in Figs. 10a and 10b. We observe that the energy harvesting rates exhibit spatial variation. To determine whether there is any correlation in harvesting rates between the two nodes, we use the Spearman rank correlation coefficient [25] given by

$$r_s = 1 - \frac{6 \sum_{i=1}^{n} d_i^2}{n(n^2 - 1)} \tag{4}$$

  where d_i is the difference between the ranks assigned to variables X and Y and n is the number of pairs of data. An r_s value of 1 indicate perfect correlation while an r_s value of close to zero would conclude that the variables are uncorrelated. Since there are 6 pairs of data, the critical value of r_s at 5% significance level is 0.829 obtained from statistical tables. The values of r_s for the outdoor and the indoor solar energy harvesters are 1.00 and 0.60 respectively. This means that the readings between nodes for the outdoor energy harvesters are correlated while that for indoor

solar energy harvesters are not strongly correlated. This is because for the outdoor energy harvester, the energy source is mainly from the sun while for indoor energy harvesters, there are many sources of energy from various fluorescent lamps in the room therefore readings are less likely to be correlated.

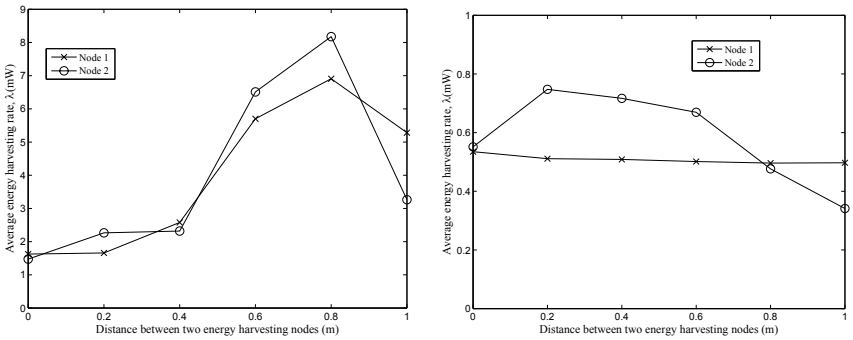

(a) Sun (b) Fluorescent lamp

Figure 10: Average charging times of nodes in the same region

- **Time correlation:**

  For each scenario, we compute the autocorrelation values for charging times recorded in different charging intervals. Figure 11 shows the results for the various scenarios. The autocorrelation values lie between -1 and 1 with 0 indicating no correlation, 1 indicating perfect correlation and -1 indicating perfect anti-correlation. The four horizontal lines indicate 95% and 99% confidence intervals for the correlation tests. From the graphs, we observe that the charging time in different intervals are either uncorrelated or weakly correlated, depending on the scenario and the time interval.

From the experimental results, we can conclude the energy harvesting rate of each node depends on the energy harvester used (indoor solar, outdoor solar or thermal), the location of the energy harvester as well as the time of the day (for outdoor solar cells).

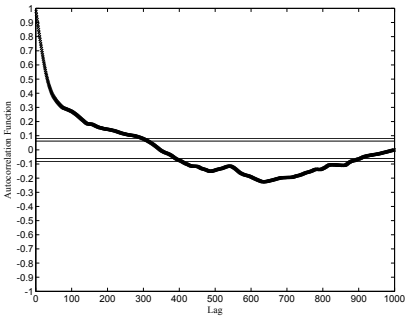

(a) Outdoor solar energy harvester at 10am

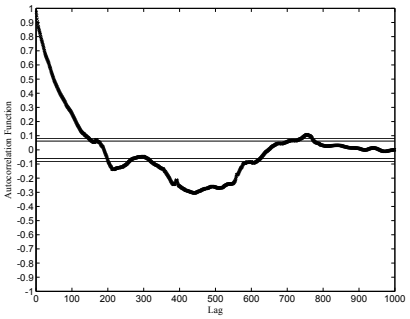

(b) Outdoor solar energy harvester at 11am

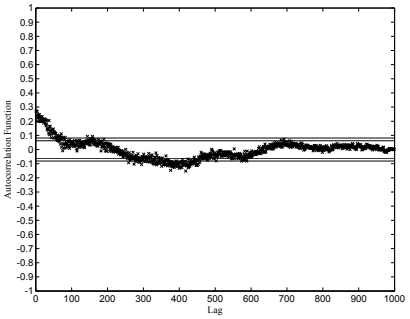

(c) Solar energy harvester directly under fluorescent lamp

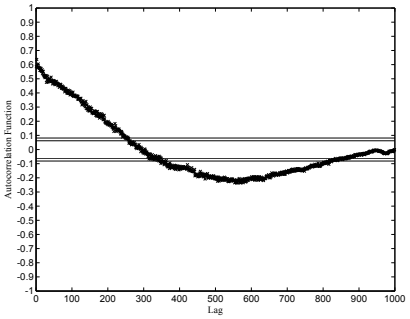

(d) Solar energy harvester 1m under fluorescent lamp

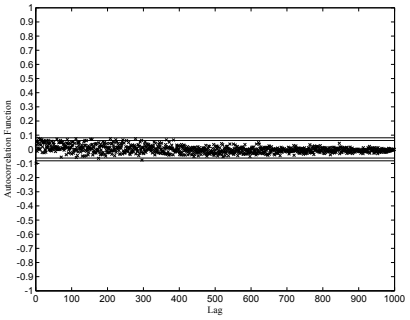

(e) Solar energy harvester 2m under fluorescent lamp

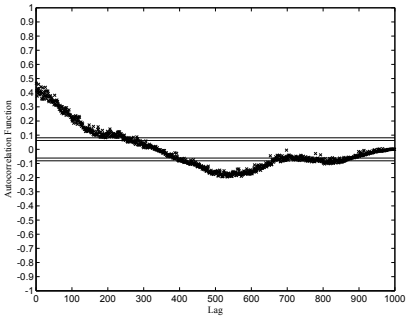

(f) Thermal energy harvester on a CPU heat sink

Figure 11: Autocorrelation function of charging times in different scenarios

4. MAC for WSN-HEAP

In this section, we begin by defining a realistic deployment scenario as well as traffic and energy model for WSN-HEAP according to the results in Section 3. Next, we define performance metrics for evaluating the efficacy of MAC protocols for active monitoring applications using WSN-HEAP. Following this, we describe CSMA-based and polling-based MAC protocols for WSN-HEAP.

4.1. Deployment Scenario

In [4], a network architecture consisting of one sink with many WSN-HEAP nodes is proposed for structural health monitoring. This type of architecture is the focus of this paper. We consider a single-hop network scenario consisting of n WSN-HEAP nodes that can transmit data directly to a sink, which is a data collection point which is connected to power mains, and therefore does not need to be charged. Based on an empirical maximum transmission range of 70m (c.f., Section 3.1), we consider a 50m by 50m deployment area for the WSN-HEAP.

4.2. Traffic and Energy Model

Unlike event-driven monitoring applications (e.g. intrusion detection) where data dissemination is only triggered upon the detection of abnormalities, sensed data is continuously being disseminated periodically to the sink. In the case of WSN-HEAP, this occurs whenever sufficient energy has been accumulated in the node. In this paper, we have used a charge-and-spend strategy where the node will go into receive state immediately after enough energy has been accumulated. While there are other energy models (e.g. duty cycling in [26]) possible, we adopt this model because

- it is simple to implement in practice. The node will monitor its energy storage and once the accumulated energy crosses the threshold, the node will turn on its processor and transceiver. This reduces the complexity of the circuit required compared to other energy models that may require more complex energy management schemes.

- the capacity of the energy storage device is limited, therefore excess harvested energy is wasted if they cannot utilized. A charge-and-spend strategy will minimize this problem.

- the delay will be minimized since a data packet will be sent to the sink once enough energy is accumulated. This is especially important for real-time monitoring or target-tracking applications where the time in which the data is sent to the sink is crucial. These applications include fire monitoring or intruder detection systems where the sensor data becomes less useful over time.

- we do not need to predict the amount of energy that can be harvested in future. This reduces computational costs as well as prediction errors when the actual amount of harvested energy is more or less than the predicted amount of harvested energy, leading to sub-optimal performance.

- we can reduce leakage by minimizing the amount of stored energy in the energy storage device as measured in [27], therefore this is beneficial to use the harvested energy once enough energy has been accumulated.

To maximize the availability of monitoring system, we attempt to transmit only one data packet in each cycle instead of multiple packets. Accordingly, our traffic and energy model is shown in Fig. 12.

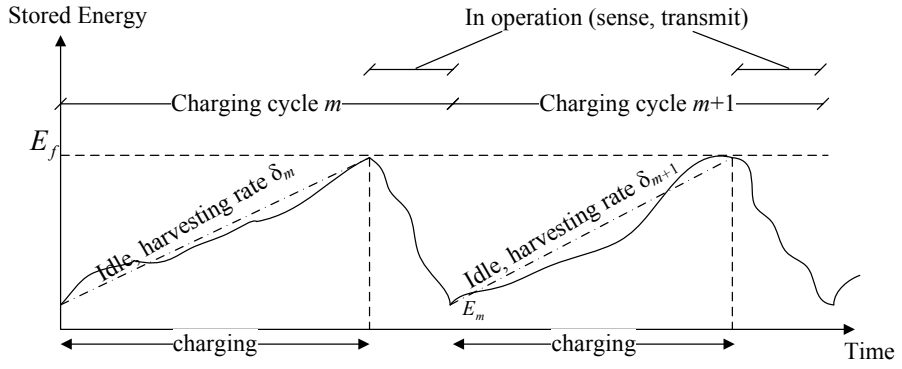

Figure 12: Energy model of a WSN-HEAP node

We model the energy charging time in each charge cycle, i.e., the time needed to charge up the capacitor to the required energy level (E_f) as a continuous and independent random variable. We evaluate the average energy harvesting rate, λ, according to the values in Table 3 as follows:

The current draw for the node is 24.2 mA and 27.9 mA for receiving and transmitting (at 1dBm) respectively as measured in [28] while the output voltage is 3 V. Accordingly, the power consumption for reception and transmission are $P_{rx} = 72.6$ mW and $P_{tx} = 83.7$ mW respectively.

4.3. Performance Metrics

A MAC protocol determines how the common wireless medium is shared among all the WSN-HEAP nodes. To compare the performance of different MAC protocols that are used in WSN-HEAP, we have identified three important performance metrics which are the network throughput (S), fairness index (F) and inter-arrival time (γ). We define R_i to be the rate of data packets received from sensor node i. S is defined to be the rate of data packets received from the sink and computed using

$$S = \sum_{i=1}^{n} R_i.$$

Our analysis assumes that packet losses are only due to collisions between two or more sending nodes and not due to poor channel conditions. Therefore, the throughput obtained from the analysis is an upper bound on the actual throughput possible since there would be packet losses due to weak signals when the channel conditions are poor. While high R and S are important in the evaluation of any MAC protocol, achieving high fairness is also essential for active monitoring applications to ensure that sensed data from every sensor is received by the sink in sufficient quantities to be analyzed. We quantify this using Jain's fairness metric [29], which is defined as

$$F = \frac{(\sum_{i=1}^{n} R_i)^2}{n(\sum_{i=1}^{n} R_i^2)}. \tag{5}$$

F is bounded between 0 and 1. If the sink receives the same amount of data

from all the sensor nodes, F is 1. If the sink receives data from only one node, then $F \to 0$ as $n \to \infty$.

Unlike traditional wireless sensor networks where users can specify a specific data packet sending rate, packets can only be sent when the WSN-HEAP node has accumulated enough energy. Therefore, the inter-arrival time, γ, of the successive data packets from each source depends on the charging characteristics of the energy harvesters.

4.4. Slotted CSMA for WSN-HEAP

We first consider a modified version of a slotted CSMA protocol which is used in IEEE 802.11 [30] and 802.15.4 [31] networks. In the slotted CSMA model, there are three states in which a node could be in, as illustrated by the state transition diagram in Fig. 13a. They are the *charging*, *carrier sensing* and *transmit* states. In the charging state, the processor and transceiver of the node are powered down to accumulate energy. In the carrier sensing (transmit) state, the processor is active and the transceiver is in receive (transmit) mode.

In the slotted form of the CSMA protocol, we denote the hardware turnaround time from receive to transmit and vice versa by t_{rx_tx} and t_{tx_rx} respectively. We define the hardware turnaround time, t_{ta}, as the larger of t_{rx_tx} or t_{tx_rx}, i.e.,

$$t_{ta} = \max(t_{rx\_tx}, t_{tx\_rx}).$$

We let the duration of each slot be t_s where $t_s = t_{ta} + t_{tx}$. A sensor would only transmit its data packet when the ongoing transmission in the current slot has ended. If there is no transmission in the current slot by any sensor, the sink would transmit a synchronization packet in that slot. To simplify our analysis, we set the size of the synchronization packet such that the end of transmission time of the synchronization packet coincides with the end of that slot. The data transmission timings are illustrated in Fig. 13b which shows that data are sent by the sensors in the 1^{st}, 2^{nd} and 4^{th} transmission slots while the sink would transmit a synchronization packet in the 3^{rd} and 5^{th} slots once it detects no sensor has transmitted in that slot. The time taken to determine whether the

channel is idle or not when it transits into the carrier sensing state is denoted by t_{cca}.

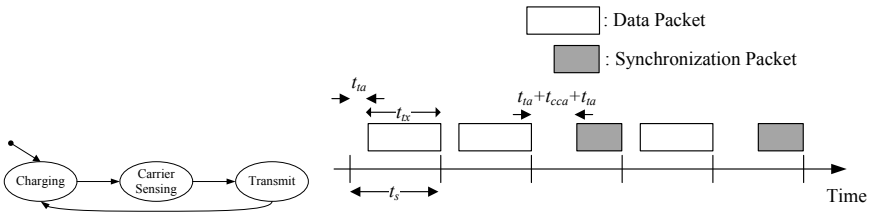

(a) State transition diagram (b) Transmission timings

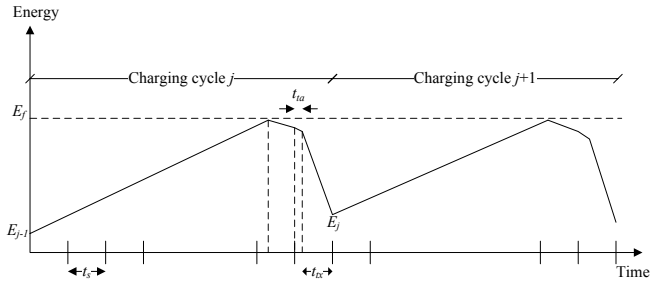

(c) Energy model

Figure 13: Slotted CSMA protocol

A cycle starts when the sensor goes into the charging state and ends when it leaves the transmit state. When the stored energy of the sensor reaches a predetermined amount of energy denoted by E_f, it wakes up and goes into the carrier sensing state to wait for the start of the next time slot. At the beginning of the next time slot, it will go into the transmit state and start sending its sensed data to the sink. This is illustrated in Fig. 13c.

From our analysis in [22], if the average energy harvesting rate for all nodes is λ, the per-node throughput, R, is given by:

$$R = \frac{\lambda[(0.5t_s + t_{cca})P_{rx} + E_{ta} + E_{tx} - \lambda t_s]^{n-1}}{[(0.5t_s + t_{cca})P_{rx} + E_{ta} + E_{tx}]^n}, \tag{6}$$

from which the network throughput is given by:

$$S = \frac{n\lambda[(0.5t_s + t_{cca})P_{rx} + E_{ta} + E_{tx} - \lambda t_s]^{n-1}}{[(0.5t_s + t_{cca})P_{rx} + E_{ta} + E_{tx}]^n}. \tag{7}$$

Finally, the inter-arrival time is given by:

$$\gamma = \frac{1}{R} \tag{8}$$

4.5. Unslotted CSMA for WSN-HEAP

Another variant of CSMA protocols is the unslotted version where transmissions do not have to be aligned to slots. For the unslotted CSMA protocol, there are five states in which a sensor could be in as illustrated by the state transition diagram in Fig. 14a. They are the *charging*, *carrier sensing*, *receive*, *idle* and *transmit* states. Initially, the sensor is uncharged so it would be in the charging state. When the energy stored reaches E_f, it goes into the carrier sensing state to determine whether the channel is free. If the channel is free, it transmits the data packet. Then, it moves into the receive state to wait for an acknowledgment (ACK) packet of size s_{ack} from the sink. After receiving the ACK packet from the sink, it returns to the charging state. Fig. 14c illustrates the energy model for a successful data transmission if the channel is free at the first carrier sensing attempt.

If the channel is busy, it performs a backoff and goes back into the charging state. If the energy stored reaches E_f but the sensor has not reached the end of its backoff period, then it remains in the idle state until the end of the backoff period, after which it goes into the carrier sensing state. The energy model when backoffs are needed is shown in Fig. 14d. The average backoff period is doubled under two situations as shown in the flowchart in Fig. 14b. The first situation is when it senses that the channel is not free. The second situation is when it does not receive an ACK from the sink after transmitting a data packet. The average backoff time is doubled after every backoff attempt by increasing the backoff exponent (BE) until it reaches $maxBE$. Each backoff duration ranges from one unit backoff period to a maximum of 2^{maxBE} unit backoff periods. Each unit backoff period is 320 microseconds which is the duration of a time slot specified in IEEE 802.15.4 standards [31]. In each backoff period, the node would be recharged until sufficient energy (E_f) is accumulated.

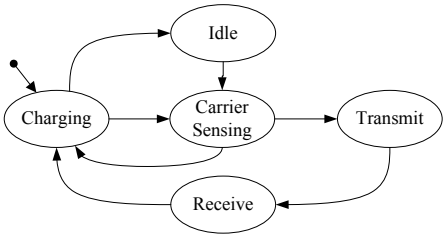

(a) State transition diagram

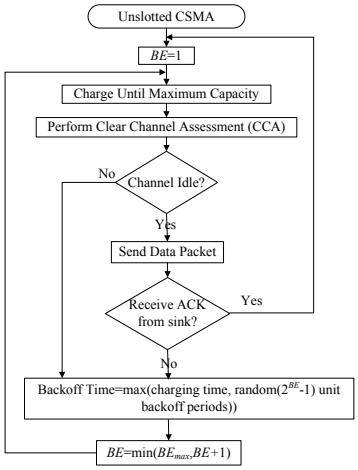

(b) Flowchart illustrating backoff mechanism

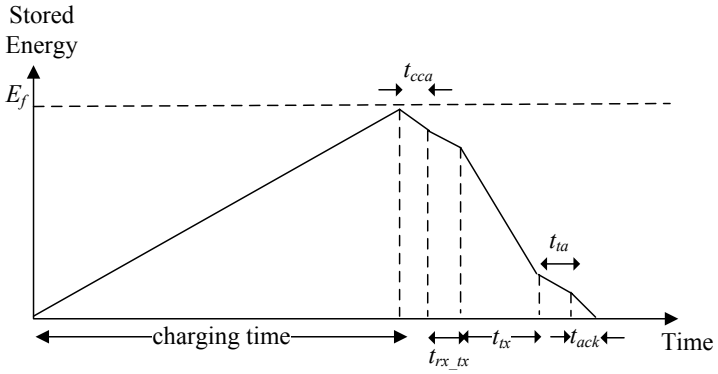

(c) Energy model of a successful transmission

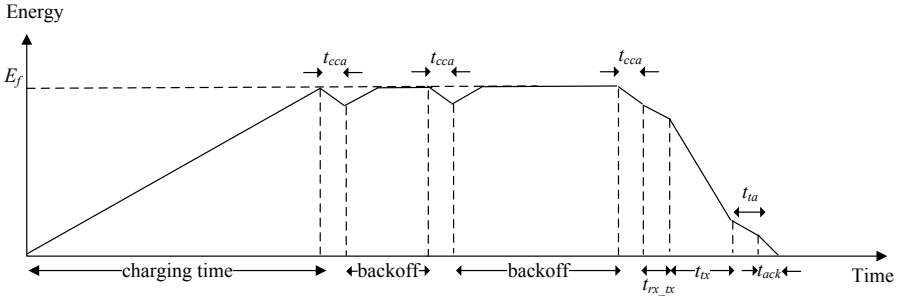

(d) Energy model when backoff periods are required

Figure 14: Unslotted CSMA protocol

4.6. ID Polling for WSN-HEAP

Polling is a common MAC protocol used in single-hop wireless networks comprising a sink and sensor nodes which are assigned a unique ID each. The sink will transmit a polling packet containing the ID of the sensor to be polled, and the polled sensor will respond with a packet transmission. If the sink can anticipate the state of the sensor, it can determine the polling ID based on a predictable schedule. However, as shown in Section 3, the energy charging times exhibit large fluctuations and are uncorrelated in both time and space. Hence, in this paper, the polling ID is randomly chosen from the set of all n nodes.

If the sensor being polled is in the receive state, it will send its sensed data to the sink after it receives the polling packet. However, it will not be polled again in the next poll since it will be in the charging state, and the sink will not be able to get a response. The state transition diagram as shown in Fig. 15a is similar to that of the slotted CSMA protocol. However, there is a new possible transition from the receive state to the charging state since the sensor has to recharge if its ID does not match the ID values in the polling packets it receives in the receive period.

Each polling packet is separated from a data packet by t_{ta} which is the time required for the sink and the polled sensor node to change states. For an unsuccessful poll, there is a minimum separation of $(2t_{ta} + t_{cca})$ between two successive polling packets which is the time required to determine whether there is any response from the sensor before another polling packet is sent, as illustrated in Fig. 15b. If the sensor is not being polled by the sink and its energy level falls below the energy required to transmit one packet, the sensor will need to harvest additional energy until the total energy reaches E_f. The energy model is illustrated in Fig. 15c.

From our preliminary work in [22], the per-node network throughput is given by

$$R = \frac{p_{rx}}{n[T + p_{rx}t_{tx} + (1 - p_{rx})t_{cca}]}. \tag{9}$$

where $T = t_{poll} + 2t_{ta}$, t_{poll} is the time taken to transmit a polling packet of size

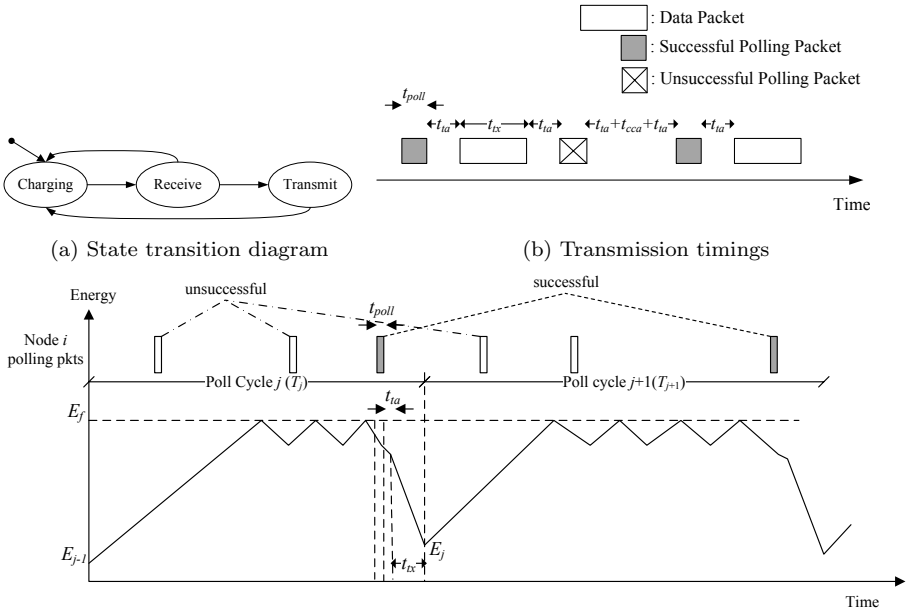

(a) State transition diagram

(b) Transmission timings

(c) Energy model

Figure 15: ID Polling

s_p and p_{rx} is the probability that the node receives a polling packet (i.e., it is in the receive state). The detailed derivation of p_{rx} is given in [22]. However, for large n and average energy harvesting rate λ, p_{rx} can be approximated by:

$$p_{rx} = \frac{\lambda}{P_{rx}} \times \frac{t_{poll} + 2t_{ta} + t_{tx}}{2t_{poll} + 2t_{ta} + t_{tx}} \tag{10}$$

The network throughput and inter-arrival time can be computed using $S = nR$ and $\gamma = \frac{1}{R}$ respectively.

Unlike slotted CSMA, the network throughput for ID polling is *independent* of n when n is large. However, if $\lambda << P_{rx}$, the achievable throughput is very small. This is because the probability of a successful poll is small since the time in which a sensor spends in receive state is much shorter than the time in charging state. Another drawback of ID polling is that the sink has to know the unique IDs of all the sensors in the network which may not be possible if we allow new nodes to be added or failed nodes to be removed over time.

5. Probabilistic Polling for WSN-HEAP

5.1. Probabilistic Polling Protocol Description

We propose to address the drawbacks of ID polling by designing a probabilistic polling protocol that *adapts* to the energy harvesting rates and/or the number of nodes in WSN-HEAP to achieve high throughput, fairness and scalability.

In probabilistic polling, instead of having the sensor's unique ID in the polling packet, the sink sets a contention probability, p_c, in the polling packet to indicate the probability that a sensor should transmit its data packet. Upon receiving the polling packet, a node would generate a random number $x \in [0, 1]$. The sensor transmits its data packet if $x < p_c$; otherwise, it will either remain in the receive state or transit to the charging state when its energy falls below the energy required to transmit one data packet. Ideally, only *one* out of all the sensors that are in receive state when polled should transmit a data packet. Accordingly, the value of p_c is updated as follows:

1: Send a polling packet with contention probability p_c.
2: **if** no sensor responds to the polling packet **then**
3: increase p_c
4: **else if** a data packet is successfully received from one of the sensor nodes or there is a packet loss due to a weak signal received from a single node **then**
5: maintain p_c at current value
6: **else if** there is a collision between two or more sensor nodes as indicated by a corrupted data packet **then**
7: decrease p_c
8: **end if**
9: Repeat step 1.

The algorithm has to differentiate between packet losses due to collision or packet error due to weak signals. This can be done using the method described in [32] which uses error patterns within a physical-layer symbol in order to expose statistical differences between collision and weak signal based losses.

The contention probability, p_c, is adjusted dynamically as follows: Since the data packet is usually larger than the polling packet, a collision will take longer than an unsuccessful poll when no node responds to the polling packet. Therefore, it would be better to increase the contention probability gradually when polling is unsuccessful and decrease the contention probability by a larger amount whenever there are collisions. Hence, an additive-increase multiplicative-decrease (AIMD) protocol is ideal for our case and we show in our performance evaluation that AIMD gives higher throughput than other schemes like multiplicative-increase multiplicative-decrease (MIMD), additive-increase additive-decrease (AIAD) and multiplicative-increase additive-decrease (MIAD).

Consequently, node additions or failures as well as changes in the energy harvesting rates are implicitly managed: When more nodes are added, the contention probability will decrease so as to reduce the number of collisions. When

there are node failures or removal of nodes from the networks, the contention probability will increase. Similarly, when the average energy harvesting rates increase (decrease), the contention probability will decrease (increase).

5.2. Analysis of probabilistic polling

When the contention probability is estimated accurately, probabilistic polling can achieve high throughput by reducing the number of collisions.

Lemma 1. The optimal contention probability that maximizes throughput is $\frac{1}{n_{active}}$ where $n_{active}(n_{active} \geq 1)$ is the number of nodes which receive the polling packet.

Proof. There can be different outcomes when a polling packet is transmitted to all its active neighbors. The probability of different outcomes can be derived analytically. We let n_{active} be the number of active neighbors which receive the polling packet (i.e. they are not in the charging state). We let W be the number of nodes which transmits a data packet when the active nodes receive the data packet. The probability of a successful transmission is

$$\begin{aligned} P(W=1) &= \binom{n_{active}}{1} p_c (1-p_c)^{(n_{active}-1)} \\ &= n_{active} p_c (1-p_c)^{(n_{active}-1)}. \end{aligned} \tag{11}$$

The probability that no node responds to the polling packet is

$$P(W=0) = (1-p_c)^{n_{active}}. \tag{12}$$

The probability of a collision is

$$P(W>1) = 1 - P(W=0) - P(W=1).$$

To maximize throughput, we would want to maximize (12). To determine the optimal value of p_c, we evaluate $\frac{dP(W=1)}{dp_c} = 0$ and get

$$n_{active}(1-p_c)^{n_{active}-1} - (n_{active}-1)p_c(1-p_c)^{n_{active}-2} = 0$$

After rearranging the terms, the optimal contention probability, p_{opt} is given by

$$p_{opt} = \frac{1}{n_{active}}. \tag{13}$$

■

We evaluate the various probability by varying the number of active nodes as shown in Fig. 16.

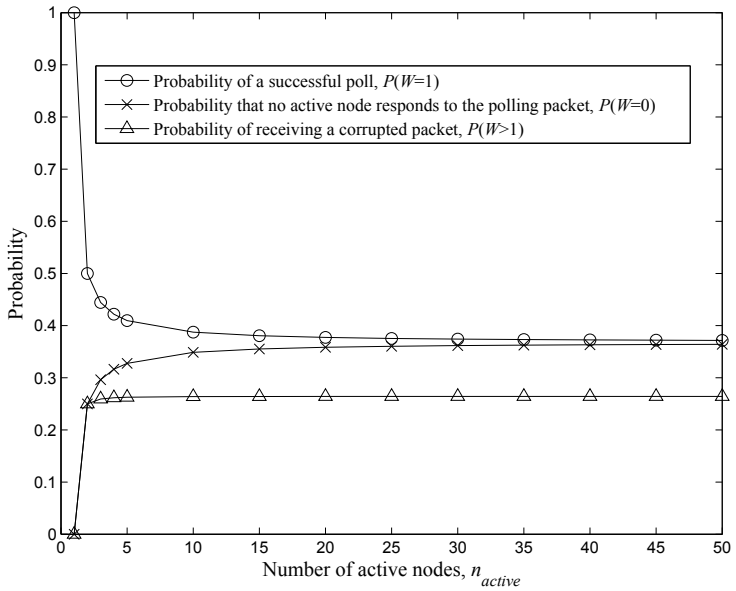

Figure 16: Probability of different outcomes for a polling attempt

Lemma 2. If the optimal contention probability is used and there are no losses due to poor channel conditions, then the probability of a successful poll is always larger than the probability of not receiving any response from a node or an unsuccessful poll due to collision between two or more sending nodes for large values of n_{active}.

Proof. We find the limits of the probability of different outcomes. By substi-

tuting (13) into (11) and taking limits,

$$\lim_{n_{active}\to+\infty} P(W=1) = \lim_{n_{active}\to+\infty} \left(1-\frac{1}{n_{active}}\right)^{(n_{active}-1)}$$
$$= \frac{\lim_{n_{active}\to+\infty}\left(1-\frac{1}{n_{active}}\right)^{n_{active}}}{\lim_{n_{active}\to+\infty}\left(1-\frac{1}{n_{active}}\right)}$$

Since $\lim_{x\to+\infty}(1-\frac{1}{x})^x = \frac{1}{e}$ and $\lim_{x\to+\infty}(1-\frac{1}{x}) = 1$,

$$\lim_{n_{active}\to+\infty} P(W=1) = \frac{1}{e} \approx 0.368$$

Similarly, by substituting (13) into (12) and taking limits,

$$\lim_{n_{active}\to+\infty} P(W=0) = \lim_{n_{active}\to+\infty} \left(1-\frac{1}{n_{active}}\right)^{n_{active}} = \frac{1}{e} \approx 0.368$$

Therefore,

$$\lim_{n_{active}\to+\infty} P(W>0) = 1 - \lim_{n_{active}\to+\infty} P(W=0) - \lim_{n_{active}\to+\infty} P(W=1)$$
$$= 1 - \frac{2}{e} \approx 0.264$$

■

This analysis shows that the minimum success probability is at least 36.8% even when the number of active nodes is large and up to 100% for low number of active nodes. Even though the probability of not receiving any data packet is up to 36.8%, this is less of a problem than packet collision since the size of the polling packet is much smaller than that of a data packet and another polling packet can be sent once a node senses that there are no data transmissions from neighboring active nodes. For the worst case scenario when there is data packet collision, this happens in at most 26.4% of the time.

5.3. Throughput Analysis of Probabilistic Polling

We derive the throughput of probabilistic polling based on the node density, energy harvesting rate as well as the contention probability adjustment scheme

used. We let p_i be the contention probability for the i^{th} polling packet sent by the sink, and let it be initialized to p_{ini}, i.e.,

$$p_1 = p_{ini}.$$

We let p_{lin} to be the linear factor, p_{mi} ($p_{mi} > 1$) be the multiplicative-increase factor and p_{md} ($p_{md} < 1$) be the multiplicative-decrease factor. Therefore, we have

$$p_{inc} = \begin{cases} p_{lin} & \text{for AIMD and AIAD} \\ (p_{mi} - 1)p_i & \text{for MIMD and MIAD} \end{cases}$$

and

$$p_{dec} = \begin{cases} p_{lin} & \text{for AIAD and MIAD} \\ (1 - p_{md})p_i & \text{for AIMD and MIMD} \end{cases}$$

If X is the number of nodes which are currently in the receive state, then:

$$P(X = x) = \binom{n}{x} p_{rx}^x (1 - p_{rx})^{n-x} \tag{14}$$

where p_{rx} is the probability that a node receives the polling packet.

If the number of nodes is small, then most of the harvested energy are used for the transmission of the data packets, and p_{rx} can be approximated by

$$p_{rx} = \frac{\lambda t_{poll}}{1.5 t_{poll} P_{rx} + t_{ta} P_{ta} + t_{tx} P_{tx}} \tag{15}$$

where λ is the average energy harvesting rate. If the number of nodes is high, then p_{rx} can be approximated using (10).

We let Y be the number of nodes which send a data packet to the sink in response to the polling packet. The probability that no sensor node responds to the polling packet is given by

$$P(Y = 0) = P(X = 0) + P(X = 1)(1 - p_i) + ... + P(X = n)(1 - p_i)^n. \tag{16}$$

The probability that exactly one sensor node responds to the polling packet is given by

$$P(Y = 1) = P(X = 1)p_i + \binom{2}{1} P(X = 2)p_i(1-p_i) + ... + \binom{n}{1} P(X = n)p_i(1-p_i)^{n-1}. \tag{17}$$

The probability that more than one sensor node respond to the polling packet which will result in a corrupted packet at the sink is given by

$$P(Y > 1) = 1 - P(Y = 0) - P(Y = 1). \tag{18}$$

Then, the contention probability is updated as follows:

$$p_{i+1} = \begin{cases} P(Y = 0)\min(p_i + p_{inc}, 1) + P(Y = 1)p_i + \\ P(Y > 1)(p_i - p_{dec}) & \text{for AIMD and MIMD} \\ P(Y = 0)\min(p_i + p_{inc}, 1) + P(Y = 1)p_i + \\ P(Y > 1)\max(p_i - p_{dec}, \epsilon) & \text{for AIAD and MIAD} \end{cases} \tag{19}$$

By evaluating (16), (17), (18) and (19) recursively, p_i may converge to a value if the values of p_{inc} and p_{dec} are well-chosen. If p_i converges, we let the converged value of p_i be p_{cv}. Then, assuming packet failures are *only* due to collisions and not packet errors, the network throughput can be computed using

$$S = \frac{1}{\left(1 + \frac{P(Y>1)}{P(Y=1)}\right)(t_{poll} + 2t_{ta} + t_{tx}) + \frac{P(Y=0)}{P(Y=1)}(t_{poll} + 2t_{ta} + t_{cca})}. \tag{20}$$

where $P(Y = 0)$, $P(Y = 1)$ and $P(Y > 1)$ can be computed by substituting p_{cv} into (16), (17) and (18) respectively. The lower and upper bound of the throughput can be obtained by using the values of p_{rx} calculated in (10) and (15).

The throughput for each node is S/n, therefore the inter-arrival time for data packets from each node is given by

$$\gamma = \frac{n}{S} \tag{21}$$

5.4. Optimal Polling for WSN-HEAP

While optimal polling cannot be implemented in practice, it gives us an upper bound on the maximum theoretical throughput attainable based on a polling MAC protocol. In the optimal polling scheme, the sink knows the current state (charging, receive or transmit) of every sensor node. If there is only one sensor node that is in the receive state, the sink will poll that sensor node. If

there is no sensor node that is in the receive state, the sink will defer sending a polling packet for a duration of t_{poll}. If there is more than one sensor node in the receive state, the sink will poll the sensor node that has the lowest per-node throughput so as to maximize the fairness metric. The probabilities of these different scenarios can be computed using (14). The network throughput can then be computed using

$$S = \frac{1}{(t_{poll} + 2t_{ta} + t_{tx}) + \frac{P(X=0)}{P(X>0)}(t_{poll} + 2t_{ta} + t_{cca})}. \quad (22)$$

For large n, and assuming an average energy harvesting rate of λ for all nodes, where $\lambda << P_{rx}$, the network throughput for ID and optimal polling can be written as follows:

$$\begin{aligned} S_{ID} &= \frac{p_{rx}}{T + t_{cca} + p_{rx}(t_{tx} - t_{cca})} \\ S_{Opt} &= \frac{p_{rx}}{\frac{T+t_{cca}}{n} + p_{rx}(t_{tx} - t_{cca})}. \end{aligned}$$

Hence, it is clear that for large n, S_{ID} remains constant while S_{Opt} increases for increasing n.

6. Simulation Results

6.1. Simulation scenario and parameters

To evaluate the performance of various MAC protocols as well as to validate our analysis, we use the Qualnet [33] network simulator to simulate a WSN-HEAP comprising a sink and n nodes deployed randomly over a 50m by 50m area. We consider data packet sizes (s_d) of 800 bits (100 bytes) and polling and acknowledgement packet sizes (s_p and s_{ack}) of 120 bits (15 bytes).

The carrier sensing time (t_{cca}) is 0.128 ms while the hardware turnaround time (t_{ta}) is 0.192 ms as given in the 802.15.4 [31] standards. Table 5 summarizes the parameter values used in our simulations. Each simulation point for the performance graphs is averaged over 10 simulation runs of 100 seconds each, except for short-term fairness, which is evaluated over periods of 10 seconds using different energy charging distributions as shown in Fig. 8.

Table 5: Values of various parameters used in simulation

Parameter	Value
n	ranges from 10 to 200
P_{rx}	72.6 mW
P_{ta}	78.15 mW
P_{tx}	83.7 mW
s_{ack}	15 bytes
s_d	100 bytes
s_p	15 bytes
t_{cca}	0.128 ms
t_{tx}	4.096 ms
t_{ta}	0.192 ms
λ	1-10 mW
α	250 kbps

6.2. Characterization of MAC schemes

In this section, we characterize the performance of each MAC scheme for various network sizes and energy harvesting rates. We set the average energy harvesting rate at 2 mW and vary n from 10 to 200 to determine the performance for low (0.004 node/m^2) and high (0.08 node/m^2) density sensor networks. As the average energy charging time is unlikely to be constant in real scenarios because it is dependent on environmental factors as well as the type of energy harvesters used, we need to ensure that our model is accurate for different charging rates. The range of energy harvesting rates (λ) we use are obtained from datasheets of commercial energy harvesters and empirical measurements. The thermal energy harvesters by Micropelt [24] can generate 0.23 mW to 6.3 mW. Our measurements show that energy harvesting rates range from 0.28 mW to 7.35 mW for different energy harvesters. In our simulations, the energy harvesting rates range from 1 mW to 10 mW (with $n = 100$)to take into account the different types and sizes of energy harvesters.

6.2.1. Slotted CSMA

The throughput results with the corresponding 95% confidence intervals for the slotted CSMA protocol are shown in Fig. 17a and 17b. As expected, the protocol does not scale to large number of sensor nodes and/or high energy harvesting rates due to excessive number of collisions when there are too many concurrent transmissions in a single slot. In addition, we also observe that the simulation results match our analysis well, validating our analytical model for slotted CSMA.

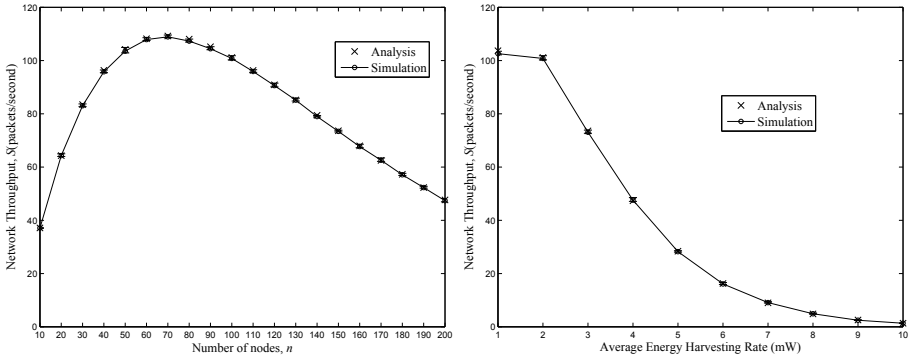

(a) Varying number of nodes (λ=2 mW) (b) Varying energy harvesting rates ($n = 100$)

Figure 17: Throughput for slotted CSMA

6.2.2. Unslotted CSMA

Next, the results for the unslotted CSMA protocol are shown in Fig. 18 for varying values of the maximum backoff exponent ($maxBE$). The performance results show that having a larger maximum backoff exponent will increase throughput when the number of nodes increases. However, the main tradeoff is that fairness will decrease since some nodes will have much lower per-node throughput compared to other nodes due to unfairness induced by the backoff mechanism. This observation is concurrent with what is observed in 802.11 wireless networks [34]. In fact, when the backoff exponent is unbounded (by assigning $maxBE$ to ∞), the throughput saturates but the fairness metric

does not converge to 1 even in the long-term. For other values of $maxBE$, the fairness metric will converge to 1 in the long-term but they induce short-term unfairness to varying degrees. We also observe that there is an optimal value of $maxBE$ that maximizes fairness for high values of n (8 in our scenario). When $maxBE$ is small, the overall throughput is low for large number of n, so the unfairness is mainly due to some nodes being starved as a result of excessive collisions. When $maxBE$ is high, the overall throughput is high and the unfairness is due to some nodes having longer backoff periods than other nodes. Therefore, there is a value of $maxBE$ that maximizes fairness when n is high depending on the type and degree of unfairness due to either excessive collisions or unequal backoff periods.

6.2.3. ID Polling

The throughput results with the corresponding 95% confidence intervals for the ID polling protocol are shown in Fig. 19. As expected, the network throughput is invariant with the network size. When we increase the energy harvesting rates, the throughput for ID polling increases as the probability of polling a sensor node increases. In addition, we also observe that the simulation results match our analysis well, validating our analytical model for ID polling.

6.2.4. Probabilistic Polling

Finally, we consider probabilistic polling. First, we validate our analytical model. The results in Fig. 20 shows that the actual throughput and inter-arrival time lies within the lower and upper bounds given by our analysis. Next, we compared AIMD scheme with other schemes (AIAD, MIAD and MIMD) using $p_{ini} = 0.01$, $p_{lin} = 0.01$, $p_{mi} = 2$, $p_{md} = 0.5$ and $\epsilon = 0.01$. The results are illustrated in Fig. 21. From the performance results, adjustment of the polling probability using the AIMD scheme outperforms other schemes which validates our motivation for using AIMD as explained in Section 5.1. We also need to determine the optimal values of p_{lin} and p_{md}. Fig. 22 shows the simulation results using different value pairs of (p_{lin}, p_{md}). If p_{lin} is too small,

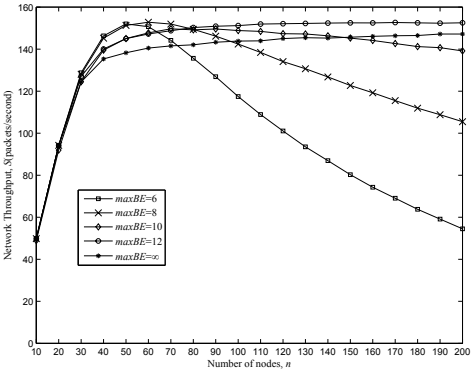

(a) Throughput

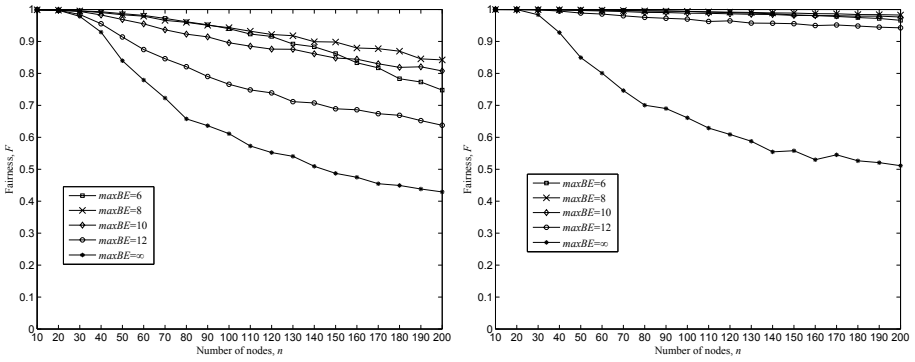

(b) Short-term Fairness

(c) Long-term Fairness

Figure 18: Throughput and fairness for varying number of WSN-HEAP nodes (n) with unslotted CSMA (λ=2 mW)

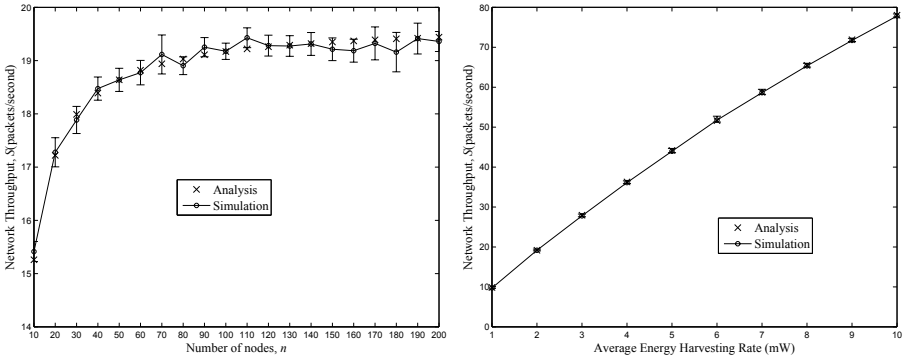

(a) Varying number of nodes (λ=2 mW) (b) Varying energy harvesting rates ($n = 100$)

Figure 19: Throughput for ID Polling

the throughput will be reduced since it would take a longer time to reach the optimal polling probability. If p_{lin} is too large, the optimal polling probability may not be reachable. Similarly, if p_{md} is too small, the decrease would be too large (since $p_{dec} = (1 - p_{md})p_i$), therefore it would take a longer time to reach the optimal probability. If p_{md} is too large, it would take many successive collisions to decrease the polling probability to the optimal range which reduces throughput.

6.3. Performance Comparison of MAC Protocols for WSN-HEAP

We have studied the performance of four MAC protocols when used in WSN-HEAP. The unslotted CSMA, slotted CSMA and ID polling protocols are modified for WSN-HEAP while probabilistic polling is designed specifically for use in WSN-HEAP. To compare the performance of these protocols with the theoretical maximum achievable, we have added the optimal polling MAC protocol for comparison. For the unslotted CSMA, we let $maxBE = \infty$ since we want to maximize throughput. The different performance metrics are illustrated in Fig. 23. The performance results show that ID polling gives consistently low throughput. This is because the probability of successfully polling a selected node is low since the node is only active for very short periods of time.

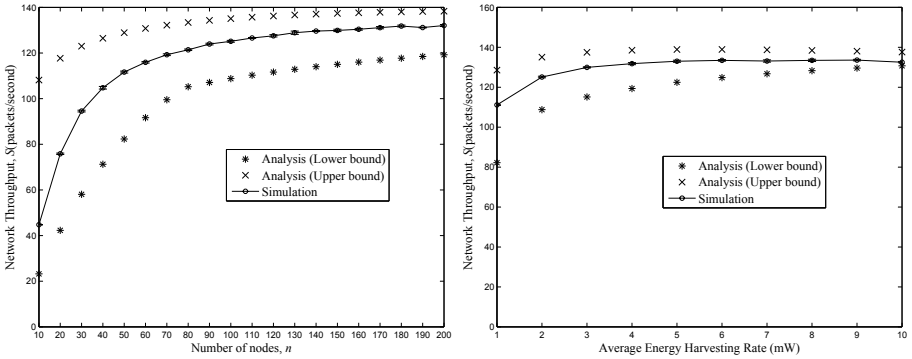

(a) Throughput for varying number of nodes (λ=2 mW)

(b) Throughput for varying energy harvesting rates ($n = 100$)

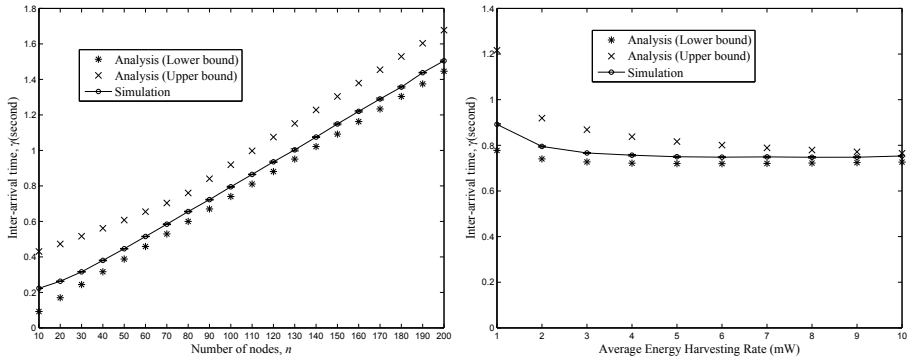

(c) Inter-arrival time for varying number of nodes (λ=2 mW)

(d) Inter-arrival time for varying energy harvesting rates ($n = 100$)

Figure 20: Throughput and inter-arrival time for probabilistic polling

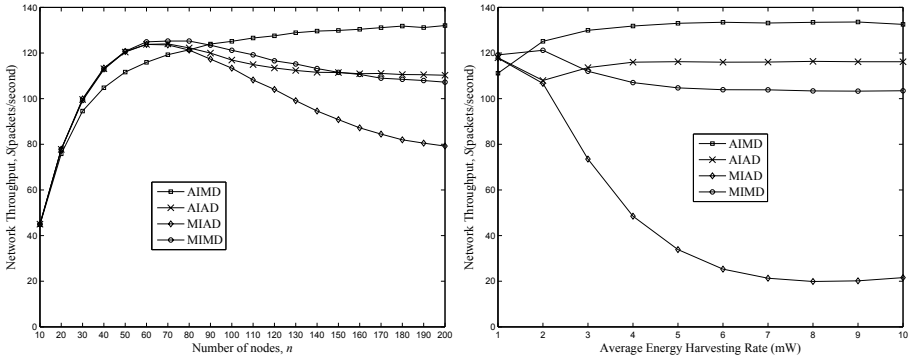

(a) Varying number of nodes (λ=2 mW) (b) Varying energy harvesting rates ($n = 100$)

Figure 21: Comparison of different contention probability (p_c) adjustment schemes for probabilistic polling ($p_{lin} = 0.01, p_{mi} = 2, p_{md} = 0.5$)

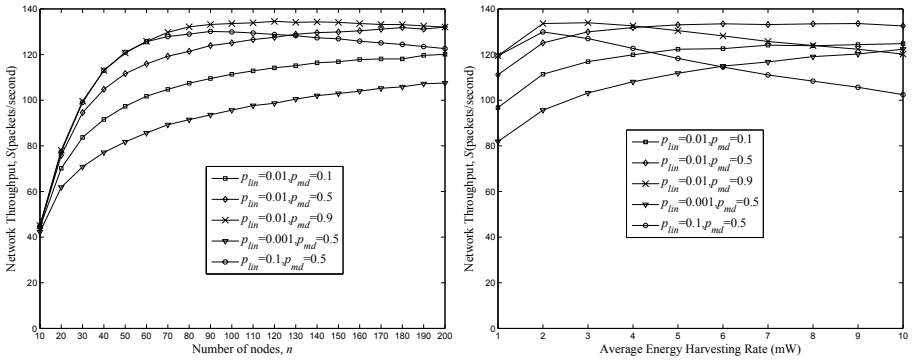

(a) Varying number of nodes (λ=2 mW) (b) Vary energy harvesting rates ($n = 100$)

Figure 22: Comparison of different parameters (p_{lin} and p_{md}) for probabilistic polling

For CSMA, the unslotted CSMA protocol outperforms the slotted version. This is due to two main factors. Firstly, for large number of WSN-HEAP nodes, the number of collisions can be reduced by having a backoff scheme. Secondly, by not having time slots, energy required is reduced during the carrier sensing state. This is because once the node senses that the channel is busy, it can go into the charging state to recharge immediately. Although unslotted CSMA gives the highest throughput in most cases, its fairness is low especially when the number of nodes is high. For probabilistic polling, the throughput is only marginally lower than that of the unslotted CSMA (for $maxBE = \infty$) but performs best among all the MAC protocols in terms of fairness. This shows that probabilistic polling is well-suited for use in WSN-HEAP to achieve high throughput and fairness.

Next, we vary the energy harvesting rates. The network throughput, short-term fairness and inter-arrival time are illustrated in Fig. 24. When the average energy harvesting rate is increased, throughput is increased because the WSN-HEAP nodes can transmit more frequently as less time is needed to harvest energy to transmit one packet. However, increased contention for the wireless channel may result in excess collisions. For the slotted CSMA protocol, throughput decreases with increasing energy harvesting rate because there is no contention resolution scheme to reduce concurrent transmissions when the average number of active nodes per time slot increases. For the unslotted CSMA, the throughput remains fairly constant because of the effectiveness of the backoff scheme in reducing contention, however the fairness is low because some nodes get to transmit more often than the others. For ID polling, throughput increases with increasing energy harvesting rate because the probability of a successful poll increases as the average charging time for each charge cycle reduces. For probabilistic polling, the contention probability acts as an effective contention resolution scheme as it can adapt to the number of active nodes. The contention probability decreases (increases) as the number of active nodes increases (decreases). Furthermore, the fairness is high as every active node has equal probability of responding to the polling packet. From the performance

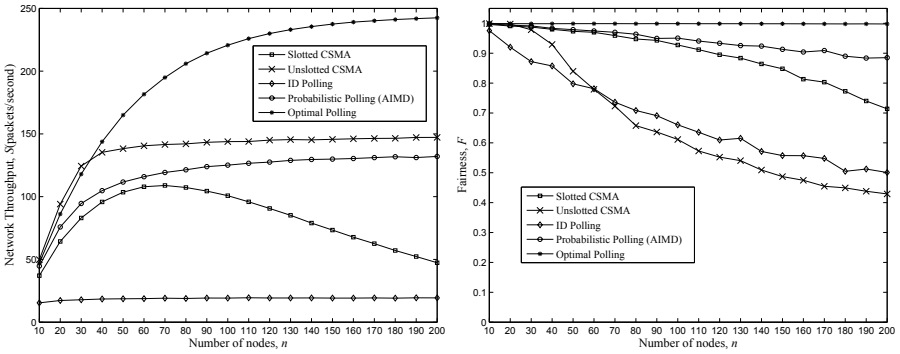

(a) Throughput (b) Short-term fairness

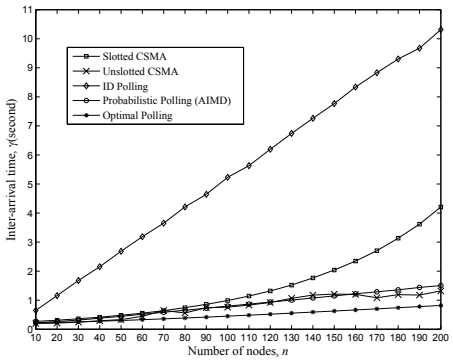

(c) Inter-arrival time

Figure 23: Performance metrics for varying number of WSN-HEAP nodes (n) for different MAC schemes (λ=2 mW)

analysis, probabilistic polling MAC protocol can give high throughput and fairness as well as low inter-arrival times when we increase the energy harvesting rates.

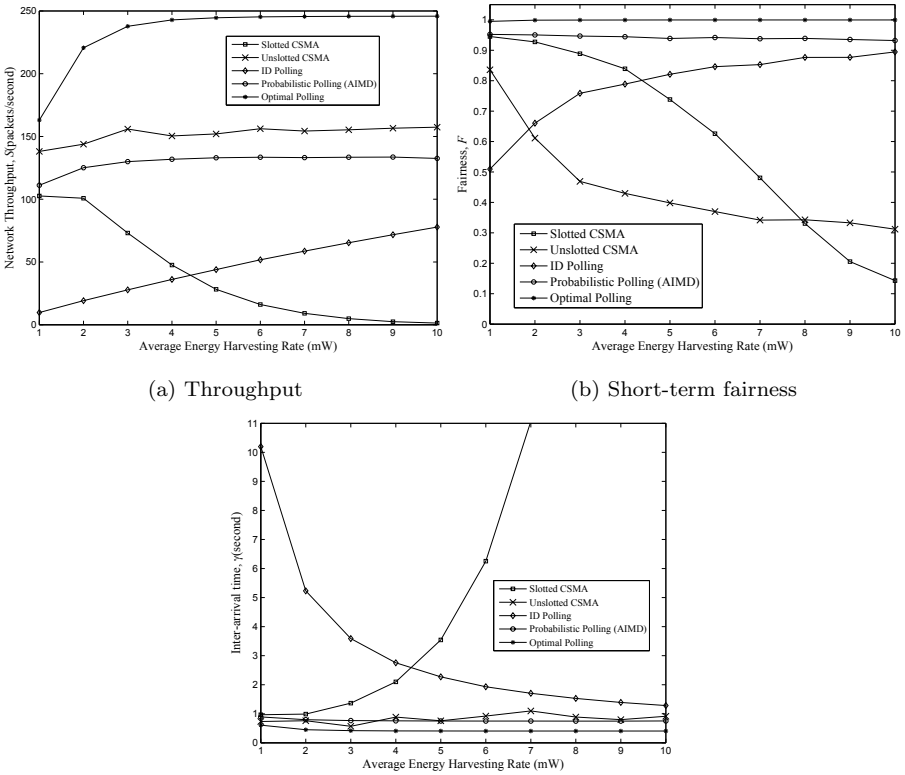

(a) Throughput

(b) Short-term fairness

(c) Inter-arrival time

Figure 24: Performance metrics for varying energy harvesting rates for different MAC schemes with 100 nodes ($n = 100$)

7. Conclusion and Future Work

Wireless sensor networks that are powered by ambient energy harvesting (WSN-HEAP) is a promising technology for many sensing applications as this eliminates the need to replace batteries as well as the need for battery disposal, which is detrimental to our environment. However, the current state of energy

harvesting technology is unable to provide a sustained energy supply to power WSNs continuously given the size constraints of the energy harvester in the sensor node, therefore WSN-HEAP can only be active for short periods of times. Moreover, the charging times are unpredictable as shown in our experimental results, making the use of many existing MAC protocols designed for WSN unsuitable or non-optimal when used in WSN-HEAP.

In this paper, we studied different MAC protocols that can be used in WSN-HEAP. We presented analytical models for the slotted CSMA, identity polling, probabilistic polling and optimal polling MAC schemes. We also derived the performance metrics, sensor and network throughput, as functions of the number of sensor nodes, charging rate, transmission time, transmit power and receive power. This gives us insights on how the performance metrics are affected by different parameters. Our analytical models were validated using simulations developed on the QualNet simulator using energy charging characteristics of commercially available energy harvesting sensor nodes. Table 6 summarizes the behavior of various MAC protocols in WSN-HEAP.

Table 6: Comparison between different MAC protocols

Property	Slotted CSMA	Unslotted CSMA	ID Polling	Probabilistic Polling
Does the protocol gives high throughput?	Only for low number of nodes	Only for large backoff window sizes	No	Yes
Does the protocol gives high fairness?	Only for low number of nodes	Only for small backoff window sizes	No	Yes
Scalability (i.e. throughput does not decrease when n increases)	No	Only for unlimited backoff window size	Yes	Yes

The evaluation results show that probabilistic polling, specially designed using the energy characteristics of WSN-HEAP nodes, gives high throughput and fairness while having low inter-arrival times and therefore is suitable to be used in WSN-HEAP. Furthermore, probabilistic polling is scalable to very high number of nodes, making it suitable to be deployed in dense sensor networks.

For future work, we are developing multi-hop MAC protocols for WSN-HEAP to support the use of multi-hop routing protocols so as to extend the range of WSN-HEAP.

[1] J. Yick, B. Mukherjee, D. Ghosal, Wireless sensor network survey, Computer Networks Journal 52 (12) (2008) 2292–2330.

[2] I. F. Akyildiz, T. Melodia, K. R. Chowdhury, A Survey on Wireless Multimedia Sensor Networks, Computer Networks Journal 51 (4) (2007) 921–960.

[3] G. Anastasi, M. Conti, M. D. Francesco, A. Passarella, Energy conservation in wireless sensor networks: A survey, Ad Hoc Networks Journal 7 (3) (2009) 537–568.

[4] G. Park, C. R. Farrar, M. D. Todd, W. Hodgkiss, T. Rosing, Energy Harvesting for Structural Health Monitoring Sensor Networks, Tech. rep., Los Alamos National Laboratory (Feb. 2007).

[5] N. Xu, S. Rangwala, K. K. Chintalapudi, D. Ganesan, A. Broad, R. Govindan, D. Estrin, A Wireless Sensor Network For Structural Monitoring, in: SenSys, 2004, pp. 13–24.

[6] M. Rahimi, H. Shah, G. S. Sukhatme, J. Heidemann, D. Estrin, Studying the feasibility of energy harvesting in a mobile sensor network, in: IEEE International Conference on Robotics and Automation (ICRA), 2003, pp. 19–24.

[7] J. A. Paradiso, T. Starner, Energy Scavenging for Mobile and Wireless Electronics, IEEE Pervasive Computing 4 (1) (2005) 18–27.

[8] F. I. Simjee, P. H. Chou, Efficient Charging of Supercapacitors for Extended Lifetime of Wireless Sensor Nodes, IEEE Transactions on Power Electronics 23 (3) (2008) 1526–1536.

[9] P. Dutta, J. Hui, J. Jeong, S. Kim, C. Sharp, J. Taneja, G. Tolle, K. Whitehouse, D. Culler, Trio: Enabling Sustainable and Scalable Outdoor Wireless Sensor Network deployments, in: IPSN, 2006, pp. 407–415.

[10] P. Sikka, P. Corke, P. Valencia, C. Crossman, D. Swain, G. Bishop-Hurley, Wireless Adhoc Sensor and Actuator Networks on the Farm, in: IPSN, 2006, pp. 492–499.

[11] P. Corke, P. Valencia, P. Sikka, T. Wark, L. Overs, Long-Duration Solar-powered Wireless Sensor Networks, in: EmNets, 2007, pp. 33–37.

[12] S. W. Arms, J. H. Galbreath, C. P. Townsend, D. L. Churchill, B. Corneau, R. P. Ketcham, N. Phan, Energy Harvesting Wireless Sensors and Networked Timing Synchronization for Aircraft Structural Health Monitoring, in: Wireless VITAE, 2009.

[13] Microstrain.
URL `http://www.microstrain.com`

[14] S. V. Krishnamurthy, A. S. Acampora, M. Zorzi, Polling-Based Media Access Protocols for Use with Smart Adaptive Array Antennas, IEEE/ACM Trans. Netw. 9 (2) (2001) 148–161.

[15] B.-S. Kim, S. W. Kim, Y. Fang, T. F. Wong, Two-Step Multipolling MAC Protocol for Wireless LANs, IEEE J. Sel. Areas Commun. 23 (6) (2005) 1276–1286.

[16] W. Ye, J. Heidemann, D. Estrin, Medium Access Control with Coordinated Adaptive Sleeping for Wireless Sensor Networks, IEEE/ACM Transactions on Networking 12 (3) (2004) 493–506.

[17] D. Niyato, E. Hossain, A. Fallahi, Sleep and Wakeup Strategies in Solar-Powered Wireless Sensor/Mesh Networks: Performance Analysis and Optimization, IEEE Trans. Mobile Comput. 6 (2) (2007) 221–236.

[18] D. Niyato, E. Hossain, M. M. Rashid, V. K. Bhargava, Wireless Sensor Networks with Energy Harvesting Technologies: A Game-Theoretic Approach to Optimal Energy Management, IEEE Wireless Commun. Mag. 14 (4) (2007) 90–96.

[19] Y. C. Tay, K. Jamieson, H. Balakrishnan, Collision-Minimizing CSMA and Its Applications to Wireless Sensor Networks, IEEE JSAC 22 (6) (2004) 1048–1057.

[20] X. Shen, W. Zhuang, H. Jiang, J. Cai, Medium Access Control in Ultra-Wideband Wireless Networks, IEEE Trans. Veh. Technol. 54 (5) (2005) 1663–1677.

[21] J. Lei, R. Yates, L. Greenstein, A Generic Model for Optimizing Single-Hop Transmission Policy of Replenishable Sensors, IEEE Trans. Wireless Commun. 8 (2) (2009) 547–551.

[22] Z. A. Eu, W. K. G. Seah, H.-P. Tan, A Study of MAC Schemes for Wireless Sensor Networks Powered by Ambient Energy Harvesting, in: Fourth International Wireless Internet Conference (WICON), 2008.

[23] MSP430 Solar Energy Harvesting Development Tool (eZ430-RF2500-SEH) from Texas Instruments.
URL `http://www.ti.com`

[24] Micropelt Thermogenerator.
URL `http://www.micropelt.com`

[25] R. E. Walpole, R. H. Myers, S. L. Myers, K. Ye, Probability & Statistics for Engineers & Scientists, Seventh Edition (2002).

[26] A. Kansal, J. Hsu, S. Zahedi, M. B. Srivastava, Power Management in Energy Harvesting Sensor Networks, ACM Transactions on Embedded Computing Systems 6 (4).

[27] T. Zhu, Z. Zhong, Y. Gu, T. He, Z.-L. Zhang, Leakage-Aware Energy Synchronization for Wireless Sensor Networks, in: MobiSys, 2009, pp. 319–332.

[28] T. Watteyne, eZWSN: Experimenting with Wireless Sensor Networks using the eZ430-RF2500 (2008).
URL `http://cnx.org/content/col10684/1.10/`

[29] R. Jain, D. M. Chiu, W. Hawe, A quantitative measure of fairness and discrimination for resource allocation in shared computer system, Tech. Rep. DEC-TR-301, Digital Equipement Corp (Sep. 1984).
URL `http://www.cs.wustl.edu/jain/papers/fairness.htm`

[30] 802.11 Stds, Wireless LAN Medium Access Control (MAC) and Physical Layer (PHY) Specifications (2003).

[31] 802.15.4-2006 Stds, Wireless Medium Access Control (MAC) and Physical Layer (PHY) Specifications for Low-Rate Wireless Personal Area Networks (WPANs) (2006).

[32] S. Rayanchu, A. Mishra, D. Agrawal, S. Saha, S. Banerjee, Diagnosing Wireless Packet Losses in 802.11: Separating Collision from Weak Signal, in: IEEE INFOCOM, 2008.

[33] Qualnet network simulator.
URL `http://www.scalable-networks.com`

[34] K. Medepalli, F. A. Tobagi, Towards Performance Modeling of IEEE 802.11 based Wireless Networks: A Unified Framework and its Applications, in: IEEE INFOCOM, 2006.